

# A new measurement of the bulk flow of X-ray luminous clusters of galaxies

A. Kashlinsky<sup>1</sup>, F. Atrio-Barandela<sup>2</sup>, H. Ebeling<sup>3</sup>, A. Edge<sup>4</sup>, D. Kocevski<sup>5</sup>

## ABSTRACT

We present new measurements of the large-scale bulk flows of galaxy clusters based on 5-year WMAP data and a significantly expanded X-ray cluster catalogue. Our method probes the flow via measurements of the kinematic Sunyaev-Zeldovich (SZ) effect produced by the hot gas in moving clusters. It computes the dipole in the cosmic microwave background (CMB) data at cluster pixels, which preserves the SZ component while integrating down other contributions. Our improved catalog of over 1,000 clusters enables us to further investigate possible systematic effects and, thanks to a higher median cluster redshift, allows us to measure the bulk flow to larger scales. We present a corrected error treatment and demonstrate that the more X-ray luminous clusters, while fewer in number, have much larger optical depth, resulting in a higher dipole and thus a more accurate flow measurement. This results in the observed correlation of the dipole derived at the aperture of zero monopole with the monopole measured over the cluster central regions. This correlation is expected if the dipole is produced by the SZ effect and cannot be caused by unidentified systematics (or primary cosmic microwave background anisotropies). We measure that the flow is consistent with approximately constant velocity out to at least  $\simeq 800$  Mpc. The significance of the measured signal peaks around  $500 h_{70}^{-1}$  Mpc, most likely because the contribution from more distant clusters becomes progressively more diluted by the WMAP beam. We can, however, at present not rule out either that these more distant clusters simply contribute less to the overall motion.

---

<sup>1</sup>SSAI and Observational Cosmology Laboratory, Code 665, Goddard Space Flight Center, Greenbelt MD 20771; alexander.kashlinsky@nasa.gov

<sup>2</sup>Fisica Teorica, University of Salamanca, 37008 Salamanca, Spain

<sup>3</sup>Institute for Astronomy, University of Hawaii, 2680 Woodlawn Drive, Honolulu, HI 96822

<sup>4</sup>Department of Physics, University of Durham, South Road, Durham DH1 3LE, UK

<sup>5</sup>Department of Physics, University of California at Davis, 1 Shields Avenue, Davis, CA 95616

*Subject headings:* Cosmology - cosmic microwave background - observations - diffuse radiation - early Universe

The large-scale isotropy of the Universe and the small-scale inhomogeneities that evolved into galaxies are thought to originate during inflationary expansion in the early Universe. Inflation posits that the primeval space-time was inhomogeneous and this structure should have been preserved on sufficiently large scales. At minimum large-scale peculiar velocities should arise from gravitational instability caused by mass inhomogeneities seeded during the inflationary expansion. On scales  $\gtrsim 100\text{Mpc}$  the standard inflationary scenario leads to robust predictions for these velocities. There the initial Harrison-Zeldovich slope of the mass fluctuations is preserved, so peculiar velocities induced by gravitational instability must decrease linearly with scale (e.g. Kashlinsky & Jones 1991); for the concordance  $\Lambda\text{CDM}$  model  $V_{\text{rms}} \sim 250(\frac{100h^{-1}\text{Mpc}}{d})$  km/sec at  $d > 50\text{--}100h^{-1}$  Mpc.

Our discovery of a coherent large-scale flow of galaxy clusters with significantly larger amplitude than expected out to  $\simeq 300\text{Mpc}$  (Kashlinsky et al 2008, 2009 – KABKE1,2) represents a challenge to the gravitational instability paradigm. Such a "dark flow" could indicate a tilt created by the pre-inflationary inhomogeneous structure of space-time (Turner 1991, Grishchuk 1992, Kashlinsky et al 1994, KABKE1) and might provide an indirect probe of the Multiverse. Various explanations have been put forward, including that the flow points to a higher-dimensional structure of gravity (Afshordi et al 2009, Khoury & Wyman 2009), or that it reflects the pre-inflationary landscape produced by certain variants of string cosmology (Mersini-Houghton & Holman 2009, Carrol et al 2008).

Making use of an expanded cluster catalog and deeper WMAP observations, we have worked to verify, and expand the Dark Flow study through a program we have dubbed *SCOUT* (**S**unyaev-Zel'dovich **C**luster **O**bservations as probes of the **U**niverse's **T**ilt). First results from this experiment are reported here.

## 1. Data and analysis

KABKE1,2 and this work utilize a method of Kashlinsky & Atrio-Barandela (2000, hereafter KA-B), which measures CMB dipole at the locations of X-ray clusters. When averaged over many isotropically distributed clusters moving at a significant bulk flow with respect to the CMB, the kinematic term dominates the SZ signal, thereby enabling a measurement of  $V_{\text{bulk}}$  over that distance. In Atrio-Barandela et al (2008, hereafter AKKE) we demonstrated

that 1) the thermal SZ (TSZ) signal from clusters extends well beyond the measured X-ray extent  $\Theta_X$ , and 2) the intra-cluster gas distribution is well approximated by the NFW profile (Navarro et al 1996) expected for dark matter in a  $\Lambda$ CDM model. The temperature  $T_X$  of hot gas distributed according to these profiles decreases significantly from the cluster cores to the cluster outskirts (Komatsu & Seljak 2001), consistent with current measurements (Pratt et al 2007) and numerical simulations (e.g. Borgani et al 2004). Consequently, the monopole produced by the TSZ component ( $\propto \tau T_X$ ) decreases, as we increase the cluster aperture, whereas the dipole due to the kinematic SZ (KSZ) component ( $\propto \tau$ , the optical depth due to Thomson scattering) remains measurable out to the aperture where we still detect the TSZ decrement in unfiltered maps (KABKE2). As in KABKE1,2 our dipole coefficients are normalized such that the dipole power  $C_1$  due to a coherent motion at velocity  $V_{\text{bulk}}$  is  $C_{1,\text{kin}} = T_{\text{CMB}}^2 \langle \tau \rangle^2 V_{\text{bulk}}^2 / c^2$ , where  $T_{\text{CMB}} = 2.725\text{K}$ . We adopt  $\Omega_{\text{total}} = 1$ ,  $\Omega_{\Lambda} = 0.7$ ,  $H_0 = 70h_{70}$  km/sec/Mpc.

To improve upon the all-sky cluster catalogue of Kocevski & Ebeling (2006) used by KABKE1,2, we have screened the ROSAT Bright-Source Catalogue (Voges et al. 1999) using the same X-ray selection criteria (including a nominal flux limit of  $1 \times 10^{-12}$  erg/sec, 0.1–2.4 keV) as employed during the Massive Cluster Survey (MACS, Ebeling et al. 2001), as well as the same optical follow-up strategy. Unlike MACS, we apply neither a declination nor a redshift limit though, thereby creating an all-sky list of cluster candidates that extends to three times fainter X-ray fluxes than in KABKE1,2. Optical follow-up observations of clusters identified in this manner and lacking spectroscopic redshifts in the literature (and MACS) are well underway using telescopes on Mauna-Kea/Hawai'i and La-Silla/Chile. As a result, our interim all-sky cluster catalogue currently comprises in excess of 1,400 X-ray selected clusters, *all* of them with spectroscopic redshifts. X-ray properties of all clusters (most importantly total luminosities and central electron densities) are computed as before (KABKE2). Within the same  $z$ -range ( $z \lesssim 0.25$ ) as our previous study, our new catalog comprises 1,174 clusters outside the KP0 CMB mask. To eliminate low-mass galaxy groups we require that clusters feature  $L_X \geq 2 \times 10^{43}$  erg/sec; 985 systems meet this criterion. This sample represents a significant improvement over the one in KABKE1,2 largely because of the substantial increase ( $z_{\text{median}} < 0.1$  in KABKE1,2 vs  $z_{\text{median}} \simeq 0.2$  below) in median cluster redshift and the higher fraction of intrinsically very X-ray luminous systems (Fig. 1a).

We applied this new cluster sample to the 5-year WMAP CMB data, processed as described in detail in KABKE1,2. The all-sky dipole in the foreground-cleaned maps from <http://www.lambda.gsfc.nasa.gov> was removed, and standard CMB masking was applied. We also need to remove the primary CMB fluctuations, produced at last scattering, as they are highly correlated and would contribute significantly to the measured dipole. To this

end, all maps were filtered as in KABKE1,2 with a filter that minimizes  $\langle(\delta T - \delta T_{\Lambda\text{CDM}})^2\rangle$ . The error budget associated with our filtering is discussed by Atrio-Barandela et al (2010, hereafter AKEKE).

Measurement errors were computed as in KABKE1,2 with one important correction. Although the filtering removes much of the CMB fluctuations, a residual component remains, due to cosmic variance and imperfections of the theoretical model. Since this residual is common to all WMAP bands, a component of the errors is correlated between the various DA maps. We address this issue in the following manner. For each of the eight differential assemblies (DAs) we simulate 4,000 realizations with  $N_{\text{cl}} = 100\text{--}1,000$  randomly selected pseudo-clusters outside of the cluster pixels and the CMB mask. In each realization we select the *same* pseudo-clusters for all DAs and evaluate the *mean* monopole and dipole averaged over all DAs:  $\bar{a}_0, \bar{a}_{1m}$ . For the 4,000 realizations at each  $N_{\text{cl}}$  we compute the mean and dispersion of  $\bar{a}_0, \bar{a}_{1m}$  over all the realizations. The distributions have zero mean and their dispersion gives errors which scale as  $N_{\text{cl}}^{-1/2}$ . We find to good accuracy that the distribution of the simulated dipoles (and monopoles) is Gaussian and the errors on each of the averaged dipole components are  $\sigma_{1m} \simeq 15\sqrt{3/N_{\text{cl}}}\mu\text{K}$  and on the monopole  $\sigma_0 \simeq 15\sqrt{1/N_{\text{cl}}}\mu\text{K}$  as explained in great detail in AKEKE; the errors of the  $x/z$  dipole component are slightly larger/smaller because of the Galactic mask (Fig. 1b).

## 2. Results

We used the filtered maps to compute the dipole and monopole terms,  $a_{1m}^i, a_0^i$  for each DA of the WMAP Q, V, W bands ( $i = 1, \dots, 8$ ) for clusters in cumulative redshift bins up to a given  $z$ . The results were averaged to obtain the mean values over all eight DAs,  $\bar{a}_{1m}, \bar{a}_0$ . Since the volume probed out to low  $z$  is too small for meaningful measurements, Table 1 lists results only for  $z$ -bins with sufficient signal-to-noise ratios (S/N). In KABKE1,2 we computed the dipole in progressively increasing apertures but no larger than  $30'$  to prevent geometric biases from very nearby Coma-type clusters. To further reduce any selection effect related to the apparent X-ray extent measured by ROSAT, we here impose a *constant* aperture for *all clusters* (see Table 1) and compute the dipole component for each  $z$ -bin at the constant aperture at which the monopole (initially negative because of the TSZ component) vanishes.

The improved cluster catalog allows us to extend our study to higher  $z$ , and to further test the impact of systematics. We create  $L_X$ -limited subsamples which achieves two important objectives. 1) As the  $L_X$  threshold is raised, fewer clusters remain and the statistical uncertainty of the dipole increases ( $\propto 1/\sqrt{N_{\text{cl}}(L > L_X)}$ ). If, however, all clusters are part of a bulk flow of a given velocity  $V_{\text{bulk}}$ , very X-ray luminous clusters will produce a larger

CMB dipole ( $\propto \tau V_{\text{bulk}}$ ), an effect that might overcome the reduced number statistics, giving a higher S/N in the measured dipole. 2) Since, as outlined under (1), the dipole signal should increase with cluster luminosity, whereas systematic effects can be expected to be independent of  $L_X$ , an actual observation of such a correlation would lend strong support to the validity of our measurement and the reality of the "dark flow".

Fig. 1a shows that the depth to which we probe the flow increases dramatically as the  $L_X$ -threshold is raised. Table 1 shows the results for each subsample. The monopole is strongly negative in the smallest apertures due to the dominance of the TSZ component in the central regions and the dipole is shown at the aperture where monopole vanishes. Of the three dipole components, the  $y$ -component is best determined, its value always remaining negative and its S/N increasing strongly with increasing  $L_X$ . As shown in Fig. 1c the amplitudes of the latter and of the monopole in the central parts are strongly, and approximately linearly, correlated. *This correlation provides strong evidence against unknown systematics - or primary CMB - causing our measurement.*

Table 1 quantifies our finding of a statistically significant dipole out to the largest scales probed ( $\sim 800h_{70}^{-1}\text{Mpc}$ ). In KABKE2 we discussed in detail why this dipole is unlikely to be produced by systematics; we briefly revisit the issue here: 1) At high statistical significance the dipole originates only at cluster positions, and must thus originate from CMB photons that passed through the hot intra-cluster gas. For the same reason the dipole can not be due to a residual contribution from the all-sky CMB dipole. HEALPix ANAFast routines (Gorski et al 2005), employed in the analysis, further remove any all-sky dipole before the filtered maps are produced. 2) Since the dipole is measured at zero monopole, the contributions from TSZ and other cluster emissions to the dipole are negligible. 3) The variations in the final aperture where the dipole is measured were very small in KABKE1,2, and the dipole signal remains in this work which uses a fixed aperture for *all* clusters. So the dipole is not affected by the variations in cluster  $\Theta_X$ , which in any case is much smaller than the final apertures in KABKE1,2. 4) The measured CMB quadrupole is significantly different from that of the  $\Lambda\text{CDM}$  model, so a significant part of the CMB quadrupole is not removed by our filter and could leak into other multipoles via the mask. However, we set the filter to zero at  $\ell \leq 4$  (KABKE2, AKEKE) for the final maps. More importantly, we have modified the pipeline to remove the all-sky quadrupole from the *original* maps and find no noticeable difference in the dipole computed at the cluster locations. This also removes the fully relativistic components from the local motion  $v_{\text{local}}$ , down to  $(v_{\text{local}}/c)^3$  corrections to the octupole. (5) Finally, we demonstrate that more luminous clusters make a larger, and statistically more significant, contribution to the dipole, as is expected if all clusters participate in the same flow, independent of  $L_X$ . Note also that the intra-cluster medium motions from cluster mergers have random directions and thus average down in large catalogs, contributing

negligibly to the noise budget below.

Although the final dipole is measured at zero monopole, tests of cross-talk were conducted as in KABKE2 by constructing CMB maps from TSZ and KSZ components of varying  $V_{\text{bulk}}$  using the derived catalog parameters, but randomly placed clusters. The parameters from randomly placed clusters were compared with those from the original clusters - the cross-talk effects are small with results similar to Fig. 6 of KABKE2 (AKEKE). To test the robustness further we select 4,000 random subsets of clusters within a given configuration and compute the mean dipole and its dispersion. The distribution of the dipoles is Gaussian, the dispersion scales as  $N_{\text{cl}}^{-1/2}$  and the results are consistent with all subsets of clusters moving in the same way within the estimated errors. E.g. randomly selecting 250/150  $L_X \geq 2 \times 10^{44}$  erg/sec clusters out of 322/208 at  $z \leq 0.25/0.2$  gives  $(\bar{a}_{1x}, \bar{a}_{1y}, \bar{a}_{1z}) = (3.7 \pm 1.8, -4.1 \pm 1.7, 4.2 \pm 1.5)/(3.6 \pm 2.1, -5.7 \pm 2.3, 4.5 \pm 1.9)\mu\text{K}$ .

To calibrate our dipole measurement in terms of an equivalent bulk velocity, we proceed as in KABKE2. This still suffers from a systematic bias which *overestimates* the amplitude of the velocity. More importantly, we measure the dipole from the filtered maps, and the convolution of the intrinsic KSZ signal with the filter can change the sign of the former for NFW clusters. The TSZ signal, being more concentrated as shown in Fig. 9 of KABKE2, is less susceptible to this effect. We therefore currently constrain only the axis of the motion; the direction along this axis should result from future applications of the KA-B method particularly to the 217 GHz *Planck* data, where the TSZ component vanishes and the angular resolution is  $5'$ , a good match to the inner parts of clusters at  $z \sim 0.1-0.2$ . Our present pipeline computes the cluster properties (central electron density,  $n_{e,0}$ ,  $T_X$ , core radius  $R_{\text{core}}$ ) assuming a  $\beta$ -model ( $\beta=2/3$ ). This model has been shown by us to be deficient at the cluster outskirts and must be replaced by the NFW profile (AKKE). We hope to accomplish this difficult task in the future with better CMB (Planck) and X-ray (Chandra/XMM) data. To summarize, our current calibration may *overestimate* the amplitude of the flow and, strictly speaking, we currently measure only the axis of motion. We stress, however, that the existence of the flow itself is not affected by this systematic uncertainty. We generated CMB temperatures from the KSZ effect for each cluster and estimate the dipole,  $C_{1,100}$ , contributed by each 100 km/sec of bulk-flow in each  $L_X, z$ -bin. Since the  $\beta$ -model still gives a fair approximation to cluster properties around  $\Theta_X$ , we present in Table 1 the final calibration coefficients evaluated at apertures of  $5'$  and  $\Theta_X$  in radius. When averaged over clusters of all X-ray luminosities the mean calibration is  $\sqrt{\langle C_{1,100} \rangle} \simeq 0.3\mu\text{K}$  in each of the  $z$ -bins. Within the uncertainties, the dependence of the calibration on  $L_X$  is in good agreement with the measured dipoles, particularly for the most accurately measured  $y$ -component. Table 1 also shows the mean central optical depth,  $\langle \tau_0 \rangle$ , evaluated from the cluster catalog. Its variation with  $L_X$  is also in good agreement with that of the measured dipole, which indicates that the clusters can

indeed be assumed to have similar profiles.

With the calibration factors in Table 1, our results are compatible with a consistently coherent flow at all  $z$ . Since the different cluster subsamples probe different depths ( $z_{\text{mean/median}}$ ), we proceed as follows to isolate the overall flow across all available scales: for the flow which extends from the smallest to the largest  $z$  in each  $z$ -bin, we model the dipoles as  $a_{1m}^n = \alpha_n V_m$ , where  $\alpha_n$  is the calibration constant for clusters in  $n$ -th luminosity bin. (Note that for each  $z$ -bin the luminosity bins are statistically independent). Both  $\sqrt{C_{1,100}}$  and  $\langle\tau_0\rangle$  scale approximately linearly with the better measured dipole coefficient,  $a_{1,y}$ , as they should in case of a coherent motion; the linear correlation coefficients are  $r = 0.92/0.93$  for correlation of  $-a_{1,y}$  with columns 7/8. We then compute by regression the velocity components with their uncertainties using the  $L_X$ -divisions at each  $z$ -bin. These numbers are shown in the summary row following each  $z$ -bin quantities for  $\alpha = \sqrt{C_{1,100}}$  at  $5'$ . We also computed them for  $\alpha_n$  given by  $\sqrt{C_{1,100}}$  at  $\Theta_X$  and by  $\langle\tau_0\rangle$  in column (7) normalized to the observed mean value of  $\langle C_{1,100}\rangle$ . Both give results essentially identical to the ones shown in the Table. The latter approximation is equivalent to assuming that all clusters have universal profiles, so that the final effective optical depth is  $\propto \langle\tau_0\rangle \times (\text{reduction factor})$ . The results here are consistent with KABKE1,2 measurements on smaller scales ( $\lesssim 400\text{Mpc}$ ), which with *revised* errors become  $(\bar{a}_{1x}, \bar{a}_{1y}, \bar{a}_{1z}) = (0.7 \pm 1.2, -3.3 \pm 1.1, 0.5 \pm 1.1)/(0.6 \pm 1.2, -2.7 \pm 1.1, 0.6 \pm 1.1)$  for  $z \leq 0.2/0.3$  with  $\sqrt{C_{1,100}} \simeq 0.3\mu\text{K}$  (Table 2, KABKE2).

The dipoles are larger for greater  $L_X$  clusters consistent with the dipole originating from the bulk motion of the clusters. We note the apparent trend in the central values of the better determined  $y$ -component peaking at  $z \leq 0.16$  and decreasing towards higher  $z$ . It is likely that this decrease is due to dilution of progressively more distant clusters, as shown by their smaller monopoles. Nevertheless, it is also possible, in principle, that the flow is dominated by the  $z \leq 0.16$  clusters with the more distant clusters contributing little to the dipole.

### 3. Discussion

We find a high likelihood of the existence of a coherent bulk flow extending to at least  $z \simeq 0.2$  with an amplitude and in a direction which are in good agreement with our earlier measurements. Our result constitutes a significant improvement in that it extends our previous work to approximately twice the distance accessible to KABKE1,2, supporting their hypothesis that the flow likely extends across much (or all) of the Hubble volume. The flow's axis is also consistent with earlier measurements of the local cluster dipole (Kocevski et al. 2004) as well as with independent measurements of bulk flows on smaller scales by

Watkins et al (2009). The velocity reported there is smaller than the numbers in Table 1, although the two amplitudes agree at  $< 2\text{-}\sigma$  level. Agreement between the two sets of central values would require  $\sqrt{\langle C_{1,100} \rangle} \sim 0.4\text{-}0.5\mu\text{K}$ , or a reduction by a factor of  $\sim 2$  from unfiltered values for NFW cluster profiles. Feldman et al (2009) extend the Watkins et al analysis and find that the absence of shear in their flow at  $\lesssim 50\text{-}100\text{Mpc}$  is consistent with the KABKE1 suggestion of the attractor at superhorizon distances.

Fig. 2 displays the results obtained in this study compared to expectations from the concordance  $\Lambda\text{CDM}$  model for 95% of cosmic observers. These results cast doubt on the notion that gravitational instability from the observed mass distribution is the sole – or even dominant – cause of the detected motion. If the current picture is confirmed, it will have profound implications for our understanding of the global structure of space-time and our Universe’s place in it.

We acknowledge NASA NNG04G089G/09-ADP09-0050 and FIS2006-05319/GR-234 grants from Spanish Ministerio de Educación y Ciencia/Junta de Castilla y León.

## REFERENCES

- Afshordi, N. Geshnizjahi, G. & Khoury, J. 2009, JCAP, 8, 30
- Atrio-Barandela, F., Kashlinsky, A., Kocevski, D. & Ebeling, H. 2008, Ap.J. (Letters), 675, L57 (AKKE)
- Atrio-Barandela, F., Kashlinsky, A., Ebeling, H., Kocevski, D. & Edge, A. 2010, ApJ, submitted, arXiv:1001.1261 (AKEKE)
- Borgani, S. et al 2004, Mon. Not. R. Astron. Soc., 348, 1078
- Carrol, S. et al 2008, arXiv:0811.1086
- Ebeling, H.; Edge, A. C.; Henry, J. P., 2001, ApJ, 553, 668
- Feldman, H., Watkins, R. & Hudson, M.J. 2009, arXiv:0911.5516v1
- Gorski, K. et al 2005, Astrophys. J., 622, 759
- Grishchuk, L. P. 1992, Phys. Rev.D 45, 4717
- Kashlinsky, A., Tkachev, I., Frieman, J. 1994, Phys. Rev. Lett., 73, 1582
- Kashlinsky, A. & Atrio-Barandela, F. 2000, Astrophys. J., 536, L67 (KA-B)
- Kashlinsky, A., Atrio-Barandela, F., Kocevski, D. & Ebeling, H. 2008, Ap.J., 686, L49 (KABKE1)
- Kashlinsky, A., Atrio-Barandela, F., Kocevski, D. & Ebeling, H. 2009, Ap.J., 691, 1479 (KABKE2)
- Kashlinsky, A. & Jones, B.J.T. 1991, Nature, 349, 753
- Khoury, J. & Wyman, M. 2009, PhRevD, 80, 064023
- Kocevski, D.D., Mullis, C.R., & Ebeling, H. 2004, Astrophys. J., 608, 721
- Kocevski, D.D. & Ebeling, H. 2006, Astrophys. J., 645, 1043



- Komatsu, E. & Seljak, U. 2001, *Mon. Not. R. Astron. Soc.*, 327, 1353  
Mersini-Houghton, L. & Holman, R. 2009, *JCAP*, 2, 6  
Navarro, J.F., Frenk, C.S. & White, S.D.M. 1996, *Astrophys. J.*, 462, 563  
Pratt, G. et al 2007, *Astron. Astrophys.* 461, 71  
Turner, M. S. 1991, *Phys.Rev.*, 44, 3737  
Watkins, R., Feldman, H. A. & Hudson, M. J. 2009, *MNRAS*, 392, 743  
Voges, W. et al 1999, *A&A*, 349, 389

Table 1. RESULTS

(1)	(2)	(3)	(4)	(5)	(6)	(7)	(8)	(9)					
$z \leq$	$L_X$ -bin $10^{44}$ erg/s	$N_{\text{cl}}$	$z_{\text{mean}}/z_{\text{median}}$	$\bar{a}_{1,x}, \bar{a}_{1,y}, \bar{a}_{1,z}$ $\mu\text{K}$	$\sqrt{C_1}$ $\mu\text{K}$	$\langle\tau_0\rangle$ $\times 10^{-3}$	$\sqrt{C_{1,100}}$ $5'$	$(\mu\text{K})$ $\Theta_X$	10'	15'	$\bar{a}_0$ 20'	$(\mu\text{K})$ 25'	30'
0.12*	0.2–0.5	142	0.061/0.060	$-4.2 \pm 2.7, -0.7 \pm 2.3, 0.5 \pm 2.3$	$4.3 \pm 2.7$	2.8	0.2301	0.1942	-2.8	0.1	–	–	–
0.12	0.5–1	194	0.081/0.082	$-2.7 \pm 2.3, -2.3 \pm 2.0, 1.4 \pm 2.0$	$3.9 \pm 2.2$	3.5	0.2989	0.2561	-2.4	-1.2	-0.1	0.6	0.8
0.12	> 1	180	0.083/0.086	$4.9 \pm 2.4, -4.5 \pm 2.1, 1.5 \pm 2.0$	$6.8 \pm 2.2$	5.4	0.4610	0.3496	-11.1	-6.5	-3.1	-0.8	0.5
$d \sim 250 - 370 h_{70}^{-1} \text{Mpc}; (V_x, V_y, V_z) = (174 \pm 407, -849 \pm 351, 348 \pm 342) \times \frac{+0.3\mu\text{K}}{\sqrt{\langle C_{1,100} \rangle}} \text{ km/sec}; V_{\text{Bulk}} = (934 \pm 352) \times \frac{0.3\mu\text{K}}{\sqrt{\langle C_{1,100} \rangle}} \text{ km/sec}; (l_0, b_0) = (282 \pm 34, 22 \pm 20)^\circ$													
0.16	0.5–1	226	0.089/0.087	$-1.5 \pm 2.2, -0.6 \pm 1.9, 2.1 \pm 1.8$	$2.7 \pm 1.9$	3.5	0.2843	0.2363	-2.8	-1.8	-0.6	0.2	1.6
0.16	1–2	191	0.106/0.107	$1.9 \pm 2.3, -2.8 \pm 2.0, -0.5 \pm 2.0$	$4.1 \pm 2.2$	4.4	0.3480	0.2894	-4.9	-1.4	0.4	1.3	1.8
0.16	> 2	130	0.115/0.125	$4.2 \pm 2.8, -8.0 \pm 2.4, 4.9 \pm 2.4$	$10.3 \pm 2.5$	6.8	0.4930	0.4238	-11.7	-7.1	-2.9	-0.3	0.8
$(a) d \sim 370 - 540 h_{70}^{-1} \text{Mpc}; (V_x, V_y, V_z) = (410 \pm 379, -1, 012 \pm 326, 566 \pm 319) \times \frac{+0.3\mu\text{K}}{\sqrt{\langle C_{1,100} \rangle}} \text{ km/sec}; V_{\text{Bulk}} = (1, 230 \pm 331) \times \frac{0.3\mu\text{K}}{\sqrt{\langle C_{1,100} \rangle}} \text{ km/sec}; (l_0, b_0) = (292 \pm 21, 27 \pm 15)^\circ$													
$(b) d \sim 370 - 540 h_{70}^{-1} \text{Mpc}; (V_x, V_y, V_z) = (428 \pm 375, -1, 029 \pm 323, 575 \pm 316) \times \frac{+0.3\mu\text{K}}{\sqrt{\langle C_{1,100} \rangle}} \text{ km/sec}; V_{\text{Bulk}} = (1, 254 \pm 328) \times \frac{+0.3\mu\text{K}}{\sqrt{\langle C_{1,100} \rangle}} \text{ km/sec}; (l_0, b_0) = (293 \pm 20, 27 \pm 15)^\circ$													
0.20	0.5–1	238	0.093/0.089	$-2.5 \pm 2.1, -1.3 \pm 1.8, 1.0 \pm 1.8$	$3.0 \pm 2.0$	3.5	0.2828	0.2390	-2.9	-2.2	-1.1	-0.3	-0.2
0.20	1–2	248	0.122/0.123	$0.1 \pm 2.0, -1.8 \pm 1.8, -0.3 \pm 1.7$	$1.8 \pm 1.8$	4.4	0.3231	0.2835	-5.1	-1.8	-0.3	0.5	1.0
0.20	> 2	208	0.140/0.151	$3.6 \pm 2.2, -5.8 \pm 1.9, 4.5 \pm 1.9$	$8.1 \pm 2.0$	6.6	0.4644	0.4218	-9.3	-5.5	-1.9	0.4	1.1
$(a) d \sim 380 - 650 h_{70}^{-1} \text{Mpc}; (V_x, V_y, V_z) = (213 \pm 341, -872 \pm 294, 529 \pm 287) \times \frac{+0.3\mu\text{K}}{\sqrt{\langle C_{1,100} \rangle}} \text{ km/sec}; V_{\text{Bulk}} = (1, 042 \pm 295) \times \frac{0.3\mu\text{K}}{\sqrt{\langle C_{1,100} \rangle}} \text{ km/sec}; (l_0, b_0) = (284 \pm 24, 30 \pm 16)^\circ$													
$(b) d \sim 380 - 650 h_{70}^{-1} \text{Mpc}; (V_x, V_y, V_z) = (248 \pm 337, -880 \pm 291, 538 \pm 284) \times \frac{0.3\mu\text{K}}{\sqrt{\langle C_{1,100} \rangle}} \text{ km/sec}; V_{\text{Bulk}} = (1, 061 \pm 292) \times \frac{0.3\mu\text{K}}{\sqrt{\langle C_{1,100} \rangle}} \text{ km/sec}; (l_0, b_0) = (286 \pm 23, 30 \pm 15)^\circ$													
0.25	0.5–1	240	0.094/0.090	$-2.3 \pm 2.1, -1.1 \pm 1.8, 0.9 \pm 1.8$	$2.7 \pm 2.0$	3.5	0.2848	0.2444	-2.8	-2.1	-1.0	-0.3	-0.1
0.25	1–2	276	0.133/0.133	$-0.2 \pm 2.0, -1.4 \pm 1.7, 0.7 \pm 1.6$	$1.6 \pm 1.7$	4.4	0.3162	0.2806	-5.8	-2.3	-0.8	-0.1	0.3
0.25	> 2	322	0.169/0.176	$3.7 \pm 1.8, -4.1 \pm 1.5, 4.1 \pm 1.5$	$6.9 \pm 1.6$	6.6	0.4434	0.4160	-6.9	-4.6	-2.3	-0.6	0.2
$(a) d \sim 385 - 755 h_{70}^{-1} \text{Mpc}; (V_x, V_y, V_z) = (313 \pm 308, -707 \pm 265, 643 \pm 259) \times \frac{+0.3\mu\text{K}}{\sqrt{\langle C_{1,100} \rangle}} \text{ km/sec}; V_{\text{Bulk}} = (1, 005 \pm 267) \times \frac{0.3\mu\text{K}}{\sqrt{\langle C_{1,100} \rangle}} \text{ km/sec}; (l_0, b_0) = (296 \pm 29, 39 \pm 15)^\circ$													
$(b) d \sim 385 - 755 h_{70}^{-1} \text{Mpc}; (V_x, V_y, V_z) = (352 \pm 304, -713 \pm 262, 652 \pm 256) \times \frac{+0.3\mu\text{K}}{\sqrt{\langle C_{1,100} \rangle}} \text{ km/sec}; V_{\text{Bulk}} = (1, 028 \pm 265) \times \frac{0.3\mu\text{K}}{\sqrt{\langle C_{1,100} \rangle}} \text{ km/sec}; (l_0, b_0) = (296 \pm 28, 39 \pm 14)^\circ$													

Note. —

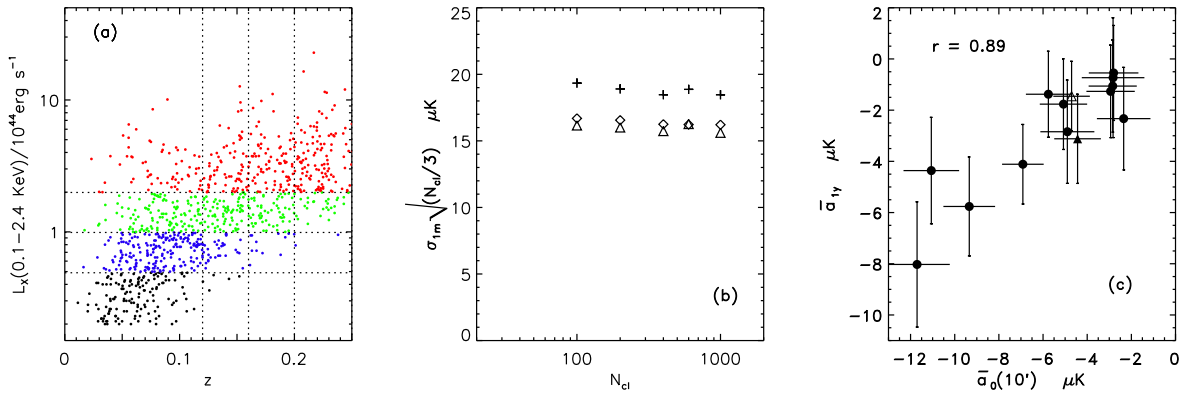


Fig. 1.—

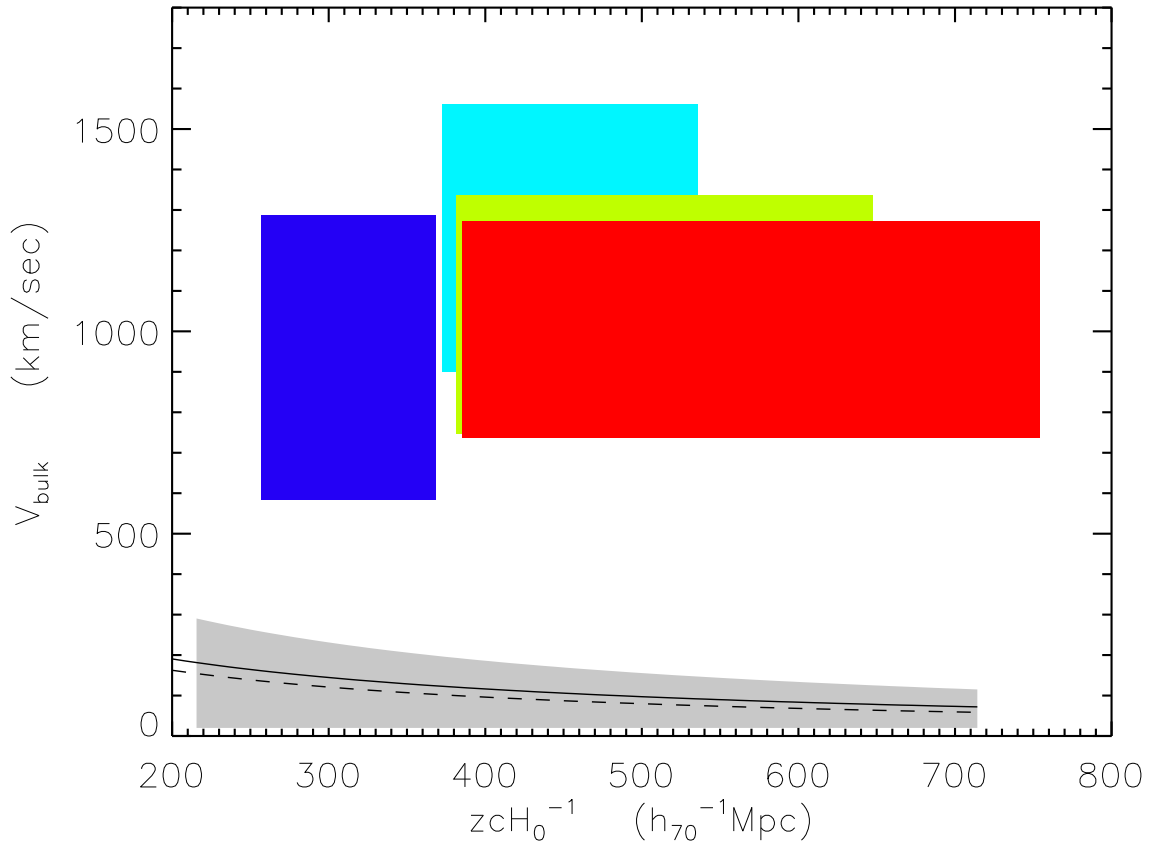


Fig. 2.—

**Figure and table captions:**

**Table 1:** : Columns are: (1) - the limit of the cumulative  $z$ -bin. (2) luminosity range of the differential  $L_X$ -bin. (3) the number of clusters per bin. (4) mean/median redshift in the bin. (5) Dipole coefficients, averaged over the eight WMAP DA's over the clusters in the bin with  $1\text{-}\sigma$  errors,  $\sigma_{1m}$ . (6) Dipole amplitude,  $\sqrt{C_1} = \sqrt{\sum_m a_{1m}^2}$ . The error on the dipole amplitude is derived as  $\sigma_1^2 = \sum_m (\partial\sqrt{C_1}/\partial a_{1m})^2 \sigma_{1m}^2 = \sum_m a_{1m}^2 \sigma_{1m}^2 / C_1$ . The binning in luminosity was designed, wherever possible, to bin different  $z$ -bins by the same luminosity range. Note that  $a_{1y}$  are always negative. When we select 598 clusters out to  $z \leq 0.25$  with  $L_X \geq 10^{44}$  erg/sec the dipoles are consistent with the brightest  $L_X$ -bin:  $(\bar{a}_{1x}, \bar{a}_{1y}, \bar{a}_{1z}) = (-0.3 \pm 1.2, -2.5 \pm 1.1, 2.4 \pm 1.1)\mu\text{K}$ . (7) Central optical depths,  $\tau_0 \equiv \sqrt{\pi}\sigma_T n_{e,0} R_{\text{core}}$ , averaged over clusters in the bin derived from our cluster catalog as described in the text. (8) Calibration factors,  $\sqrt{C_{1,100}}$ , for clusters in the given bin at  $5'$  radial distance from the cluster centers and at 1 X-ray extent for  $\beta$ -model with  $\beta = 2/3$ . (9) Measured monopole, over the fixed aperture with the radius shown, after averaging over all DA's.

The row at the end of each  $z$ -bin sums up the bulk flow parameters (scale, components, amplitude and direction to the axis of motion) assuming a coherent motion for all the  $L_X$ -bins. The depth is defined as  $d \equiv z_{\text{median}} cH_0^{-1}$ .

(\*) There are only five clusters in this  $L_X$ -range at  $z > 0.12$ , so for brevity this configuration's parameters are not repeated the remaining  $z$ -bins, although for completeness it is included in bulk flow evaluations <sup>(b)</sup>.

<sup>(a)</sup> The bulk flow is derived using column 8 parameters without the lowest  $L_X$ -clusters which do not extend beyond  $z = 0.12$  <sup>(\*)</sup> (see text).

<sup>(b)</sup> The bulk flow is derived using column 7 parameters including the lowest  $L_X$ -clusters <sup>(\*)</sup> (see text).

**Figure 1:** (a)  $z$ -distribution of clusters in the  $L_X$ -bins used in the analysis. Black/blue/green/red colors correspond to  $L_X = (0.2 - 0.5, 0.5 - 1, 1 - 2, > 2) \times 10^{44}$  erg/sec respectively. (b) Standard deviations from simulations of random pseudo-clusters vs  $N_{\text{cl}}$ . Pluses/diamonds/triangles correspond to  $a_{1x}/a_{1y}/a_{1z}$ . (c) Correlation between the  $y$ -component of the dipole and the central monopole from Table 1 (filled circles). Both quantities increase in amplitude with  $L_X$  because the optical depth and central temperature increase for more massive clusters: KSZ dipole scales as  $\tau$  and the monopole as  $\tau T_X$ . The linear correlation coefficient for the circles is shown in the upper left. Triangles correspond to differential  $z$ -configuration,  $0.12 < z \leq 0.25$ , where we still have enough luminous clusters for reasonable S/N. Open/filled triangles correspond to  $L_X > (1, 2) \times 10^{44}$  erg/sec with 418/260 clusters. When the triangles are included the linear correlation coefficient becomes 0.85.

**Figure 2:** Bulk velocity vs depth from Table 1: blue/cyan/green/red corresponds to  $z \leq 0.12/0.16/0.2/0.25$ ; parameters for fits (a) are chosen for brevity. Solid/dashed lines correspond to the rms bulk velocity for the concordance  $\Lambda$ CDM model for top-hat/Gaussian windows. Black-shaded regions shows the 95% confidence level of the model (see KABKE1 for details).